TMPRSS2:ERG Fusion by Translocation or Interstitial Deletion Is Highly Relevant in Androgen-Dependent Prostate Cancer, But Is Bypassed in Late-Stage Androgen Receptor–Negative Prostate Cancer

Karin G. Hermans,[1] Ronald van Marion,[1] Herman van Dekken,[1] Guido Jenster,[2] Wytske M. van Weerden,[2] and Jan Trapman[1]

Departments of [1]Pathology and [2]Urology, Josephine Nefkens Institute, Erasmus University Medical Center, Rotterdam, the Netherlands

Abstract

Recently, a unique fusion between the prostate-specific, androgen-regulated *TMPRSS2* gene and the ETS genes *ERG, ETV1*, or *ETV4* has been described in clinical prostate cancer. We investigated mechanisms of expression of four ETS genes, *ERG, ETV1, ETV4*, and *FLI1*, in 11 xenografts representing different stages of prostate cancer. All five androgen-dependent xenografts showed as major transcript overexpression of two splice variants of *TMPRSS2:ERG*, linking *TMPRSS2* exon 1 or 2 sequences to *ERG* exon 4. In one of two androgen-sensitive xenografts, fusion transcripts of *TMPRSS2* and *ETV1* were detected. Array-based comparative genomic hybridization and interphase fluorescence *in situ* hybridization indicated both interstitial deletions and translocations as mechanisms of *TMPRSS2:ERG* gene fusion. Importantly, *TMPRSS2* to *ERG* fusions were also observed in three of four androgen-independent, androgen receptor (AR)–negative xenografts and in two AR-negative clinical prostate cancer specimens; however, the fusion gene was not expressed. In almost all AR-negative tumor samples, overexpression of wild-type *ETV4* or *FLI1* was detected. Combined, our observations indicate a key role of fusion of *TMPRSS2* and ETS genes in most androgen-regulated prostate cancers, which might be bypassed by androgen-independent expression of wild-type ETS factors in late-stage disease. (Cancer Res 2006; 66(22): 10658-63)

Introduction

Prostate cancer is the most frequent cancer in men in countries with a Western lifestyle and the second cause of male cancer death (1). Surgery and radiation are standard therapy of localized prostate cancer. Palliative therapy of metastatic prostate cancer aims at blocking androgen receptor (AR) function. A better understanding of the molecular mechanisms of tumorigenesis is essential for the development of novel therapies. Additionally, a knowledge of the mechanism of prostate cancer development will improve prediction of the clinical course of the disease.

Recently, overexpression of the ETS gene *ERG* has been described in clinical prostate cancer (2). Subsequently, it was shown that overexpression of *ERG* and related *ETV1* was due to fusion of the *TMPRSS2* gene to either *ERG* or *ETV1* (3). This important finding adds gene fusion to the mechanisms of gene overexpression in epithelial tumors. At low frequency, *TMPRSS2* might also be fused to *ETV4* in prostate cancer (4). Expression of *TMPRSS2* that maps to 21q22 is androgen regulated and prostate specific (5). *ERG* is also located on 21q22, ~3 Mbp proximal to *TMPRSS2. ETV1* maps to 7p21 and *ETV4* to 17q21. Together with *FLI1*, modified *ERG, ETV1*, and *ETV4* are well-known oncogenes involved in translocations in Ewing sarcoma and acute myeloid leukemia (6).

We investigated the ETS genes *ERG, ETV1, ETV4*, and *FLI1* in human prostate cancers transplanted on nude mice. Xenografts are powerful models for dedicated genetic and molecular studies because they lack normal cells of human origin. The xenografts used represent a variety of clinical stages of prostate cancer, ranging from primary tumors and local metastases to recurrent disease and distant metastases, and from androgen-dependent to androgen-independent cancers (7–9). Our data reveal both interstitial deletion and gene translocation as mechanisms of fusion between *TMPRSS2* and *ERG*. Further, our results show high overexpression of two splice variants of the *TMPRSS2:ERG* fusion gene in all androgen-dependent xenografts and absence of *ERG* overexpression in late-stage, AR-negative xenografts, even if they contain a *TMPRSS2:ERG* fusion gene. The latter observation was also made in AR-negative clinical prostate cancer. In almost all late-stage, AR-negative prostate cancer samples, apparently androgen-independent expression of wild-type *ETV4* and *FLI1* is detected. These findings show a key role of *TMPRSS2:ERG* in androgen-dependent prostate cancer, which might be bypassed by other ETS factors in late-stage, AR-negative disease.

Materials and Methods

Prostate cancer samples. The *in vivo* growing xenografts PCEW, PC82, PC133, PC135, PC295, PC310, PC324, PC329, PC339, PC346, and PC374 were propagated by serial transplantation on male nude mice as described (7–9). PCEW, PC82, PC295, PC310, and PC329, derived from primary tumors or local metastases, are androgen-dependent. PC133, PC324, PC339, PC346, and PC376 are derived from distant metastases or local progressive disease and are androgen-independent (PC133, PC324, and PC339) or androgen-sensitive (PC346 and PC374). PC135 is androgen independent and is derived from a lymph node metastasis (see Supplementary Table S1).

Clinical prostate tumor samples were obtained from recurrent disease by transurethral resection (TUR-P) after informed consent, following approval of the institutional ethical committee.

DNA and RNA preparation. Genomic DNA was isolated using the Puregene system from Gentra Systems (Minneapolis, MN) according to the procedure described by the manufacturer. Xenograft RNA was isolated

Note: Supplementary data for this article are available at Cancer Research Online (http://cancerres.aacrjournals.org/).

Requests for reprints: Jan Trapman, Department of Pathology, Josephine Nefkens Institute, Erasmus University Medical Center, PO Box 2040, 3000 CA Rotterdam, the Netherlands. Phone: 31-104087933; Fax: 31-104089487; E-mail: j.trapman@erasmusmc.nl.

doi:10.1158/0008-5472.CAN-06-1871

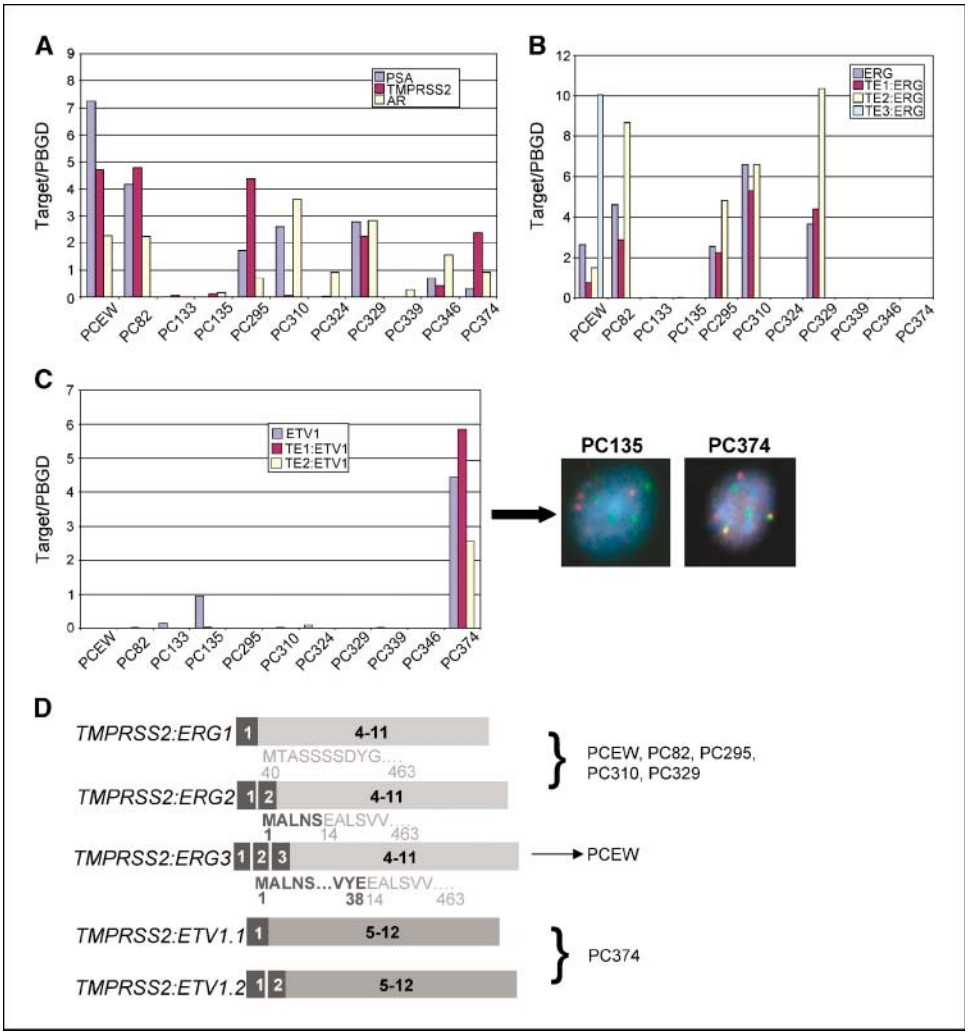

Figure 1. Expression of *AR, PSA, TMPRSS2*, and *ERG* and *ETV1* fusion transcripts in prostate cancer xenografts. *A,* QPCR of *AR, PSA*, and *TMPRSS2* mRNAs. *B,* QPCR of *ERG* and *TMPRSS2:ERG* fusion transcripts. *C,* QPCR of *ETV1* and *TMPRSS2:ETV1* fusion transcripts and interphase FISH with *TMPRSS2* (*green spots*) and *ETV1* (*red spots*) specific BACs of nuclei from PC135 and PC374. *D,* composition of *TMPRSS2:ERG* and *TMPRSS2:ETV1* fusion transcripts. Details of methods, FISH BACs, and QPCR primers are described in Materials and Methods. *PBGD* expression was used as a QPCR reference.

according to the LiCl protocol (10). For isolation of RNA from clinical samples, the Illustra mini RNA kit (General Electric Healthcare, Fairfield, CT) was used.

Array-based comparative genomic hybridization. Arrays were produced from the human 3600 bacterial artificial chromosome (BAC)/P1-derived artificial chromosome genomic clone set of the Welcome Trust Sanger Institute, covering the full genome at ~1 Mb spacing. Degenerated oligonucleotide PCR products were prepared for spotting on CodeLink slides (General Electric Healthcare) according to published protocols (11) with some modifications (12). DNA labeling and hybridization were done essentially as described (11) with minor modifications (13). After hybridization arrays were scanned in a ScanArray Express HT (Perkin-Elmer, Freemont, CA). The resulting images were analyzed with GenePix Pro 5.0 software (Axon Instruments, Foster City, CA) and subsequently visualized with an excel macro (12).

Quantitative PCR. Analysis of mRNA expression was done by quantitative PCR (QPCR). Two micrograms RNA were reverse transcribed using 400 units M-MLV RT (Invitrogen Life Technologies, Carlsbad, CA) and an oligo-dT12 primer. QPCR was done in an ABI Prism 7700 Sequence Detection System (Applied Biosystems, Foster City, CA). QPCR reactions were done in Power SYBR Green PCR Master Mix (Applied Biosystems) containing 330 nmol/L forward and reverse primer in a total volume of 25 μL. Thermocycling conditions were according to the recommendations of the manufacturer. Amounts of specific RNAs for each sample were determined relative to *posphobilinogen deaminase* (*PBDG*) by the standard curve method (Applied Biosystems). Primer combinations used were as follows: PBGD-F (5′-CATGTCTGGTAACGGCAATG-3′) and PBGD-R (5′-GTACGAGGCTTTCAATGTTG-3′). PSA-4A (5′-ACGTGTGTGCAAGTTCACC-3′) and PSA-5B (5′-TGTACAGGGAAGGCCTTTCG-3′). TMPRSS2-F (5′-CCTCTGGTCACTTCGAAGAAC-3′) and TMPRSS2-R (5′-GTAAAACGACGTCAAGGACG-3′). AR-7/8A (5′-TGACTCCGTGCAGCCTATTG-3′) and AR-8B (5′-ATGGGAAGCAAAGTCTGAAG-3′). TMPRSS2-E1:ERG-E4F (5′-AGCGCGGCAGGAAGCCTTA-3′) and ERG-E4/5R (5′-CATCAGGAGAGTTCCTTGAG-3′). TMPRSS2-E2:ERG-E4F (5′-GATGGCTTTGAACTCAGAAGC-3′) and ERG-E4/5R. TMPRSS2-E3F (5′-CCACCAGCTATTGGACCTTA-3′) and ERG-E4/5R (5′-CATCAGGAGAGTTCCTTGAG-3′). TMPRSS2-E1F (5′-GAGCTAAGCAGGAGGCGGA-3′) and ETV1-E5R (5′-TGACTGCAGGCAGAGCTGAT-3′). TMPRSS2-E2F (5′-CCTATCACTCGATGCTGT-3′) and ETV1-E5R. ERG-F (5′-TGCTCAACCATCTCCTTCCA-3′) and ERG-R (5′-TGGGTTTGCTCTTCCGCTCT-3′). ETV1-F (5′-CATACCAACGGCGAGGATCA-3′) and ETV1-R (5′-TGGAGAAAAGGGCTTCTGGA-3′). ETV4-F (5′-ACCGGCCAGCCATGAATTAC-3′) and ETV4-R (5′-GAGAGCTGGACGCTGATTG-3′). FLI1-F (5′-GAGGAGCTTGGGGCAATAAC-3′) and FLI1-R (5′-AGAGCAGCTCCAGGAGGAAT-3′).

Interphase fluorescent *in situ* hybridization. Nuclear suspensions of the prostate cancer xenografts were prepared essentially as described by Vindelov et al. (14). Interphase fluorescent *in situ* hybridization (FISH) was done as described (15). BAC clones RP11-164E1, RP5-1031F17 (both flanking *ERG*, see Fig. 2*A*), RP11-113F1 (*TMPRSS2*, see Fig. 2*A*), RP11-79G16 (*ETV1*), RP11-268E15 (*ETV4*) and RP11-44O2 (*FLI1*) were purchased from BacPac Resources (Oakland, CA). Specificity of BACs is shown in Supplementary Figs. S1 and S2. BAC DNA clones were biotin-16-dUTP or

digoxigenin-11-dUTP labeled using a nick translation reagent kit (Vysis, Downers Grove, IL) according to the directions of the manufacturer. Biotin-labeled probes were visualized with FITC-conjugated avidin (Vector Laboratory, Burlingame, CA) and digoxigenin-labeled probes with rhodamine-conjugated antidigoxigenin antibody (Roche, Mannheim, Germany). Cells were 4′,6-diamidino-2-phenylindole counterstained. Images of the three fluorochromes were collected on an epifluorescence microscope (Leica DM, Rijswijk, the Netherlands) equipped with appropriate filter sets (Leica) and a CCD cooled camera (Photometrics, Tucson, AZ).

Sequence analysis. PCR products were purified using SAP/Exonuclease I (USB Corporation, Cleveland, OH) according to the instructions of the manufacturer. Purified PCR fragments were labeled using the ABI BigDye Terminator Ready Reaction kit v3.1 (Applied Biosystems) according to instructions of the manufacturer. In the sequence reactions, the same primers were used as for fragment amplification. Sequence samples were run on the ABI 3100 genetic Analyzer (Applied Biosystems).

Results and Discussion

Eleven xenografts derived from various stages of clinical prostate cancer (Supplementary Table S1; refs. 7–9) were used to decipher the role of ETS genes. PCEW, PC82, PC295, PC310, PC329, PC346, and PC374 are AR positive. PCEW, PC82, PC295, PC310, and PC329 grow androgen dependent on male nude mice; PC346 and PC374 are, to a varying extent, androgen sensitive. PC133, PC135, PC324, and PC339 are androgen independent.

First, expression of *AR, PSA*, and *TMPRSS2* in xenografts was assessed by QPCR. There is a good correlation between the expression of *AR* and the well-known, androgen-regulated *PSA* and *TMPRSS2* genes in androgen-dependent and androgen-sensitive xenografts (Fig. 1*A*; refs. 5, 9, 16). An exception is PC310, which shows *AR* and *PSA* expression, but clearly is *TMPRSS2* negative (see below). All androgen-independent xenografts are AR negative or express an inactive AR, as deduced from lack of *PSA* and *TMPRSS2* expression (see also ref. 17).

Next, we investigated expression of *ERG* and *TMPRSS2:ERG* fusion transcripts using an *ERG* specific primer set and primer sets spanning *TMPRSS2* exons 1, 2, or 3 and *ERG* exon 4, respectively, combined with an *ERG* exon 4/5 primer (Fig. 1*B*). In all five androgen-dependent xenografts, *ERG* overexpression corresponded with *AR* and *PSA* expression, linking *ERG* to a functional AR and to strict androgen-dependent tumor growth. Overexpression of *ERG* correlated with the presence of *TMPRSS2:ERG* fusion transcripts. As confirmed by sequencing, due to alternative splicing in all five xenografts, two transcripts were present, one containing *TMPRSS2* exon 1 linked to *ERG* exon 4 and a second, linking *TMPRSS2* exons 1 and 2 to *ERG* exon 4, respectively (Fig. 1*D*). PCEW contained a third transcript linking part of *TMPRSS2* exon 3 to *ERG* exon 4 due to use of a cryptic splice donor site in *TMPRSS2* exon 3. The open reading frame (ORF) of transcript 1 is predicted to start at an internal ATG in *ERG* exon 4. In transcripts 2 and 3, the ORF will begin at the start codon of *TMPRSS2* and continues in-frame with the indicated part of *ERG* (Fig. 1*D*). The reason of the high frequency of alternative splicing is at present unclear. Possibly expression of a truncated ERG protein from the *TMPRSS2(exon 1):ERG(exon 4)* fusion transcript favors tumor growth.

Androgen-sensitive PC374 showed high *ETV1* overexpression (Fig. 1*C*). High *ETV1* expression correlated with *TMPRSS2:ETV1*

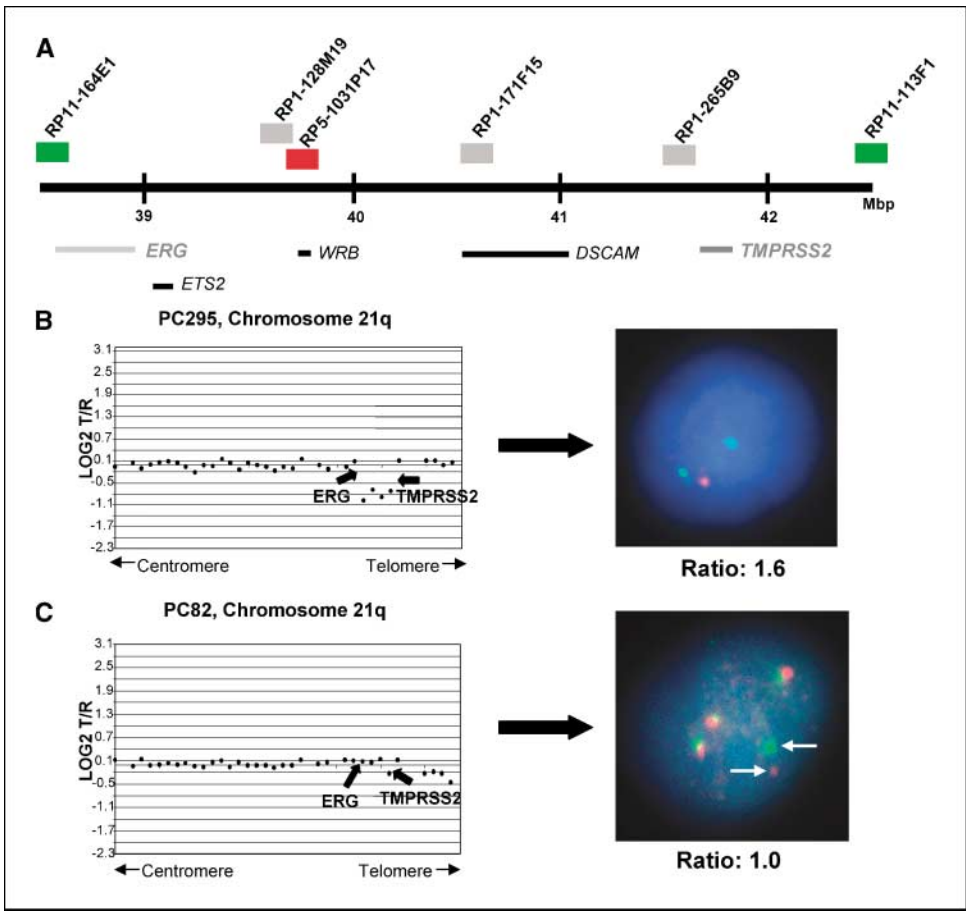

Figure 2. Array-based CGH analysis of chromosome 21 and interphase FISH of nuclei of prostate cancer xenografts PC295 and PC82. *A,* chromosome 21 region indicating the position of *ERG, TMPRSS2*, and flanking genes in Mbp from the top of the p arm. Positions of BAC clones in this region are indicated above the map. Genes mapping in this chromosomal region are indicated below the map. BACs used in interphase FISH are in red or green. *B,* PC295: array-CGH of 21q and representative interphase FISH (two *green spots* and one *red spot*) of a nucleus, using BACs RP11-164E1 (*green*) and RP5-1031P17 (*red*). *C,* PC82: array-CGH of 21q and representative interphase FISH of a nucleus, using the same BACs as above. Ratios of green to red spots in interphase FISH, as calculated from over 30 nuclei, are indicated below the pictures. *White arrows,* separate spots in the PC82 nucleus. *Black arrows,* positions of *ERG* and *TMPRSS2* in the array-CGH figures. *X axis,* log2 ratio of normalized hybridization signal of tumor DNA versus reference DNA (*T/R*).

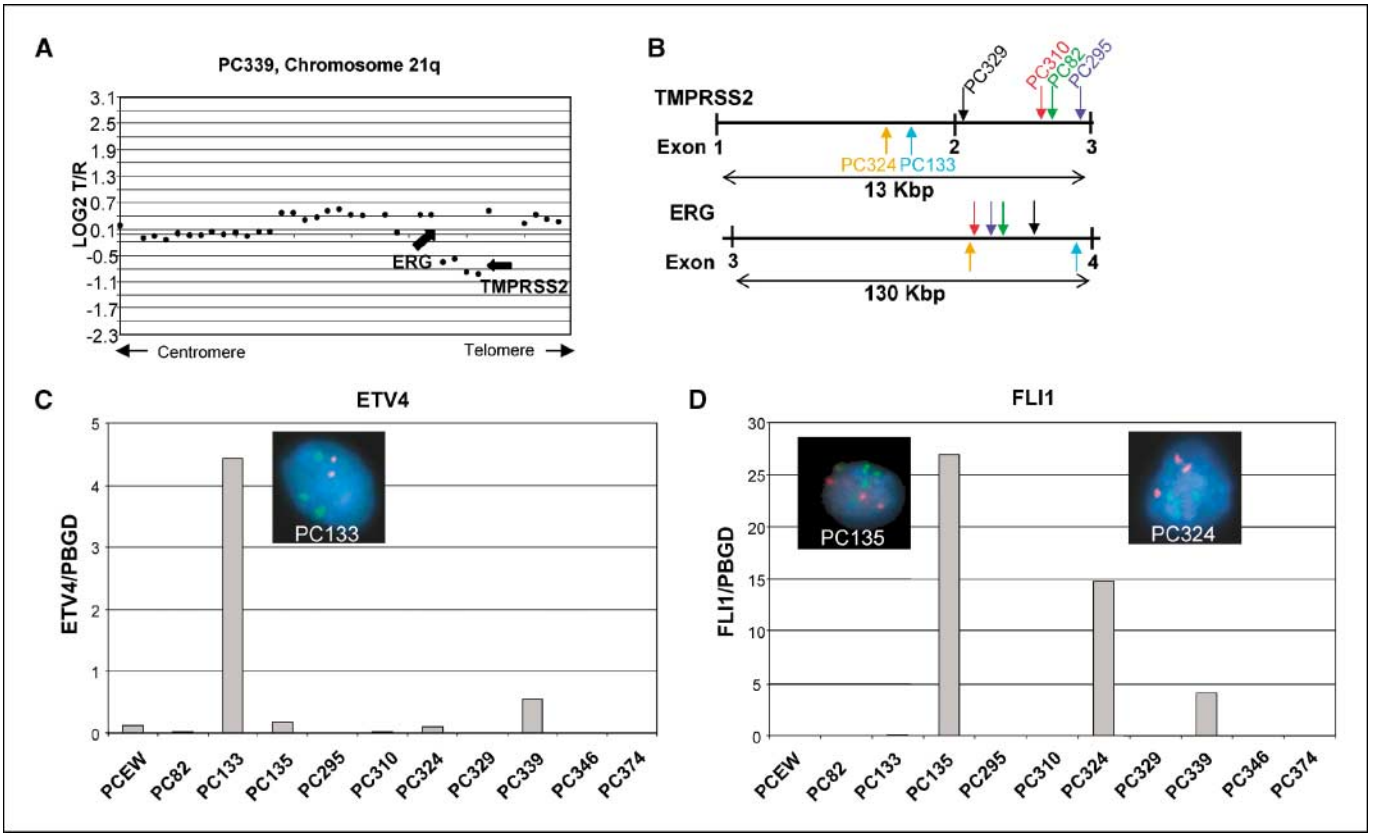

Figure 3. Genetic and expression analysis of AR-negative prostate cancer xenografts. *A,* array-CGH of chromosome 21q of androgen-independent, AR-negative xenograft PC339 (for details, see Fig. 2 and Materials and Methods). *B,* positions of breakpoints in *ERG* and *TMPRSS2* in xenograft DNAs. Breakpoints were mapped by standard long-range PCR using a mixture of Taq and Proofstart DNA polymerase, as indicated by the manufacturer (Qiagen, Valencia, CA). Above the genes, the positions of breakpoints in AR-positive, androgen-dependent xenografts are shown; below the genes, the breakpoints in AR-negative xenografts are indicated. *C,* QPCR of *ETV4* expression in prostate cancer xenografts. *D,* QPCR of *FLI1* expression in prostate cancer xenografts. Details are described in the legend to Fig. 1 and in Materials and Methods. Standard 5′-RACE, using the Generacer kit from Invitrogen, indicated that *ETV4* and *FLI1* transcripts in AR-negative PC133, PC135, PC324, or PC399 were wild type. *Insets* (*C* and *D*), representative interphase FISH pictures of nuclei from indicated xenografts, showing the absence of fusion of *TMPRSS2* to *ETV4* or *FLI1*. *Green spots, TMPRSS2* (*C* and *D*); *red spots, ETV4* (*C*) and *FLI1* (*D*).

gene fusion, as shown by interphase FISH on nuclear suspensions using *ETV1* and *TMPRSS2* specific BACs (Fig. 1*C*), and the presence of two splice variants of *TMPRSS2:ETV1* (Fig. 1*C* and *D*). *ERG* and *ETV1* were not overexpressed in PC346 or in late-stage, AR-negative prostate cancer xenografts. Interphase FISH indicated that low-level *ETV1* expression in PC135 could not be correlated with *TMPRSS2* gene fusion (Fig. 1*C*). 5′-Rapid amplification of cDNA ends (5′-RACE) confirmed that *ETV1* expressed in PC135 was wild type (data not shown).

TMPRSS2 and *ERG* map in the same orientation at short distance on chromosome band 21q22.2-q22.3 (Fig. 2*A*). To determine the mechanism of *TMPRSS2:ERG* gene fusion, genomic DNA from the five xenografts overexpressing the fusion gene was investigated by 1-Mbp-spaced array-based comparative genomic hybridization (array-CGH). Two different representative array-CGH profiles of chromosome 21 are depicted in Fig. 2*B* and *C*. In PC295, the region between *ERG* and *TMPRSS2* was lost, as indicated by the low T/R ratio of the four BACs mapping in this chromosomal region (Fig. 2*B*). A similar profile was present in PC329 (data not shown). Although PC82 contains the fusion transcript, the region between *ERG* and *TMPRSS2* was largely present (Fig. 2*C*). A comparable profile was found in PCEW and PC310 (data not shown). In PC310, the profile was accompanied by a small homozygous deletion of the last exons of *TMPRSS2* (data not shown), explaining total absence of *TMPRSS2* transcripts in this xenograft. We extended the array-CGH data by interphase FISH of PC82, PC295, and PC310 nuclei. We used as hybridization probes BACs RP11-164E1 and RP5-1031P17, which map at a distance of ~1 Mbp, flanking *ERG* at positions indicated in Fig. 2*A*. Both BACs exclusively stained chromosome band 21q22.2 and showed two spots on interphase nuclei from normal cells (Supplementary Fig. S1*A* and *B*). Representative nuclei of PC295 and PC82 are presented in Fig. 2*B* and *C*, respectively. In nuclei from PC295 cells, we found a higher number of green spots than red spots (average ratio 1.6), indicative of loss of the region between *ERG* and *TMPRSS2* in one copy of chromosome 21. In PC82 and PC310, we observed an identical number of green and red spots (average ratios 1.0 and 1.1, respectively). In PC82 that contains four copies of chromosome 21, three pairs of red and green spots were always closely linked and one pair was clearly separated, as illustrated in Fig. 2*C*. Both array-CGH and FISH data strongly suggest two different mechanisms of *TMPRSS2:ERG* fusion: one by an ~3 Mbp interstitial deletion of one copy of chromosome 21, and a second more complex mechanism by chromosomal translocation.

Array-CGH of genomic DNA from two of the six xenografts that did not overexpress *TMPRSS2:ERG* showed a remarkable pattern. In the androgen-independent, AR-negative xenografts PC133 and PC339, we detected a similar interstitial deletion as in PC295 and

PC329. The chromosome 21 profile of PC339 is depicted in Fig. 3*A*. Long-range PCR followed by sequencing confirmed the fusion between *TMPRSS2* and *ERG* in PC133, mapping the chromosomal breakpoints in *ERG* intron 3 and in *TMPRSS2* intron 1, respectively (Fig. 3*B*). Similarly, PCR plus sequencing identified *TMPRSS2:ERG* fusion in PC324 that does not show a 21q22 interstitial deletion. This adds a third AR-negative xenograft to those with *TMPRSS2:ERG* gene fusion without expression of the fusion gene. Like in PC133, the breakpoint in PC324 is in *TMPRSS2* intron 1. We also mapped the breakpoints in AR-positive PC82, PC295, PC310, and PC329 (Fig. 3*B*). As expected from expression data (Fig. 1*B*), these breakpoints were in intron 2 of *TMPRSS2* and in intron 3 of *ERG*. All six breakpoints in *ERG* were in the last part of intron 3, suggesting a preferred region of recombination in this part of the gene. It remains to be investigated whether the difference in *TMPRSS2* introns involved in *ERG* fusion between AR-positive and AR-negative xenografts, introns 2 and 1, respectively, is coincidental or of functional importance. The absence of *TMPRSS2:ERG* expression in PC133, PC324, and PC339 (Fig. 1*B*) indicates that it is not involved in the androgen-independent growth of these xenografts. Importantly, however, the presence of *TMPRSS2:ERG* in genomic DNA strongly suggests that the fusion gene has been instrumental in an earlier androgen-dependent stage of tumor growth.

We postulated that in PC133, PC324, and PC339, androgen-regulated *ERG* expression is bypassed and subsequently down-regulated by other mechanisms of progressive tumor growth. One mechanism to become independent of androgen-regulated *ERG* overexpression might be by androgen-independent increased expression of a member of the ETS transcription factor gene family. As shown in Fig. 1, we had no evidence that this was the case for *ERG* or *ETV1*. Therefore, we investigated in the xenografts expression of two other ETS transcription factors known to be involved in oncogenesis, *ETV4* and *FLI1*. *ETV4* was highly expressed in PC133 and *FLI1* in PC324 and PC135 (Fig. 3*C* and *D*). Also, in PC339, we observed expression of *FLI1*. *ETV4* and *FLI1* were not or were hardly expressed in androgen-dependent or androgen-sensitive xenografts. Overexpression was not the result of fusion to *TMPRSS2* as illustrated by interphase FISH (Fig. 3*C* and *D*). Additional 5′-RACE experiments confirmed that *ETV4* and *FLI1* mRNA in AR-negative xenografts was wild type and not the result of fusion to other genes (data not shown).

In clinical prostate cancer, many recurrent tumors still express a functional AR. However, a substantial proportion of recurrent tumors is heterogeneous for AR expression or is AR negative (18, 19). We investigated whether, like in xenografts, *TMPRSS2:ERG* gene fusion without expression of the fusion gene was present in clinical samples. Array-CGH showed in 4 of 11 recurrent tumors the interstitial deletion at 21q22 indicative of *TMPRSS2:ERG* fusion (see, e.g., Fig. 4*A* and *B*). From three of these tumors (T1-1, T1-8, and T3-7), RNA was available. Importantly, we also had available DNA and RNA from recurrent tumor T1-7 of which AR-negative xenograft PC324 was derived. These four tumors and a control recurrent tumor without *TMPRSS2:ERG* fusion (T6-9)

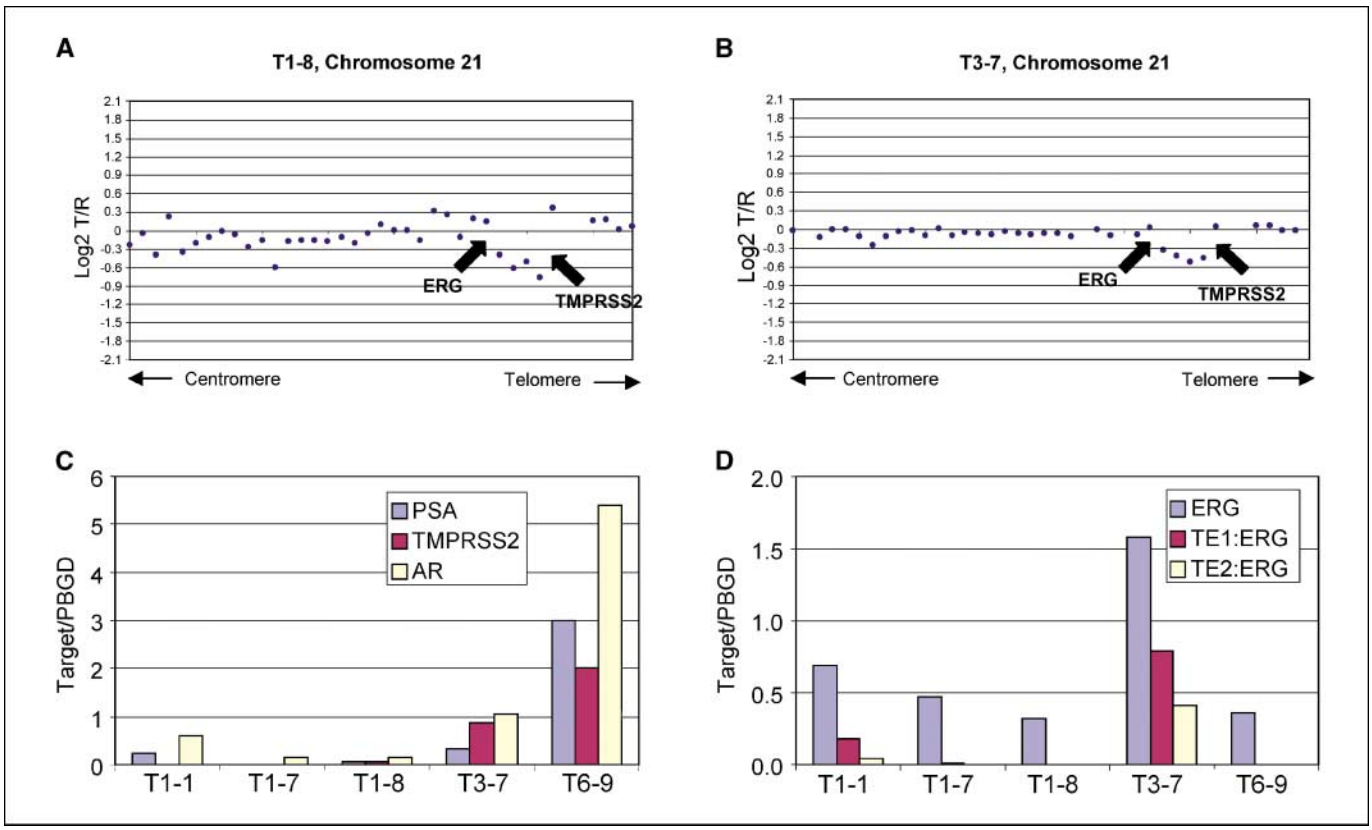

Figure 4. Array-based CGH of chromosome 21 and specific gene expression patterns of clinical recurrent prostate cancer specimens. *A* and *B,* array-CGH of chromosome 21 of recurrent tumors T1-8 and T3-7. *Black arrows,* positions of *ERG* and *TMPRSS2*. *X axis,* log2 ratio of normalized hybridization signal of tumor DNA versus reference DNA. *C,* QPCR of *AR, PSA*, and *TMPRSS2* mRNAs. *D,* QPCR of *ERG* and *TMPRSS2:ERG* fusion transcripts. Details of methods and QPCR primers are described in Materials and Methods. *PBGD* expression was used as a QPCR reference.

were investigated by QPCR for specific gene expression patterns (Fig. 4*C* and *D*). T1-1, T3-7, and T6-9 expressed *AR* and its target genes *PSA* and *TMPRSS2*, although expression in T1-1 was low. In contrast, T1-8 and, as expected, T1-7 showed hardly any *AR, PSA*, and *TMPRSS2* expression. All tumor samples had a basal level of *ERG* expression. *ERG* overexpression, combined with *TMPRSS2:ERG* fusion transcripts, was clearly detected in T3-7 and absent in T1-8 and T1-7. T1-1 showed a low level of *TMPRSS2:ERG* expression, which might indicate tumor heterogeneity. The data confirm and extend the findings in xenografts showing that AR-negative tumors can carry a *TMPRSS2:ERG* fusion gene without expression of the gene. Background expression levels and presumed heterogeneity of tumors hampered accurate investigation of *ETV4* and *FLI1* in the clinical samples (Supplementary Fig. S3). *ETV4* expression was highest in AR-negative T1-8 and T1-7, but differences with other tumor samples were small. Like in PC324, expression of *FLI1* was high in T1-7, but T1-1 also showed high expression of *FLI1*. The latter might be explained by tumor heterogeneity, as proposed previously (Fig. 4*C* and *D*). Obviously, more detailed immunohistochemical studies, including AR and ETV4 or FLI1 double staining, are needed to substantiate the latter observation.

In conclusion, our xenograft data extend previous observations in clinical prostate cancer (3, 4) and shed new light on the role of ETS transcription factors in prostate cancer. First, we detected two mechanisms of gene fusion between *ERG* and *TMPRSS2.* Second, we observed that *TMPRSS2:ERG* overexpression is functionally correlated with *AR* expression. Both in xenografts and clinical samples, we showed that the *TMPRSS2:ERG* fusion gene can be present in absence expression of the gene in AR-negative tumors. Furthermore, our data suggest that other members of the ETS family, possibly wild-type *ETV4* or *FLI1*, might take over the role of androgen-regulated *TMPRSS2:ERG* in late-stage, AR-negative prostate cancer.

Acknowledgments

Received 5/24/2006; revised 9/13/2006; accepted 10/5/2006.

Grant support: Erasmus University Medical Center and the Dutch Cancer Society (Koningin Wilhelmina Fonds).

The costs of publication of this article were defrayed in part by the payment of page charges. This article must therefore be hereby marked *advertisement* in accordance with 18 U.S.C. Section 1734 solely to indicate this fact.

References

1. Jemal A, Murray T, Ward E, et al. Cancer statistics, 2005. CA Cancer J Clin 2005;55:10–30.
2. Petrovics G, Liu A, Shaheduzzaman S, et al. Frequent overexpression of ETS-related gene-1 (ERG1) in prostate cancer transcriptome. Oncogene 2005;24:3847–52.
3. Tomlins SA, Rhodes DR, Perner S, et al. Recurrent fusion of TMPRSS2 and ETS transcription factor genes in prostate cancer. Science 2005;310:644–8.
4. Tomlins SA, Mehra R, Rhodes DR, et al. TMPRSS2: ETV4 gene fusions define a third molecular subtype of prostate cancer. Cancer Res 2006;66:3396–400.
5. Lin B, Ferguson C, White JT, et al. Prostate-localized and androgen-regulated expression of the membrane-bound serine protease TMPRSS2. Cancer Res 1999;59:4180–4.
6. Oikawa T. ETS transcription factors: possible targets for cancer therapy. Cancer Sci 2004;95:626–33.
7. Hoehn W, Schroeder FH, Reimann JF, Joebis AC, Hermanek P. Human prostatic adenocarcinoma: some characteristics of a serially transplantable line in nude mice (PC 82). Prostate 1980;1:95–104.
8. Hoehn W, Wagner M, Riemann JF, et al. Prostatic adenocarcinoma PC EW, a new human tumor line transplantable in nude mice. Prostate 1984;5:445–52.
9. van Weerden WM, de Ridder CM, Verdaasdonk CL, et al. Development of seven new human prostate tumor xenograft models and their histopathological characterization. Am J Pathol 1996;149:1055–62.
10. Sambrook J, Russell DW. Molecular cloning. A laboratory manual. 3rd ed. Cold Spring Harbor. Vol. 1. New York: Cold Spring Harbor Laboratory Press; 2001. p. 1.59–61.
11. Fiegler H, Carr P, Douglas EJ, et al. DNA microarrays for comparative genomic hybridization based on DOP-PCR amplification of BAC and PAC clones. Genes Chromosomes Cancer 2003;36:361–74.
12. Knijnenburg J, Szuhai K, Giltay J, et al. Insights from genomic microarrays into structural chromosome rearrangements. Am J Med Genet A 2005;132:36–40.
13. Verhagen P, van Duijn P, Hermans K, et al. The PTEN gene in locally progressive prostate cancer is preferentially inactivated by bi-allelic gene deletion. J Pathol 2006;208:699–707.
14. Vindelov LL, Christensen IJ, Nissen NI. A detergent-trypsin method for the preparation of nuclei for flow cytometric DNA analysis. Cytometry 1983;3:323–7.
15. van Duin M, van Marion R, Vissers K, et al. High-resolution array comparative genomic hybridization of chromosome arm 8q: evaluation of genetic progression markers for prostate cancer. Genes Chromosomes Cancer 2005;44:438–49.
16. Riegman PH, Vlietstra RJ, van der Korput JA, Brinkmann AO, Trapman J. The promoter of the prostate-specific antigen gene contains a functional androgen responsive element. Mol Endocrinol 1991;5:1921–30.
17. Hendriksen PJ, Dits NF, Kokame K, et al. Evolution of the androgen receptor pathway during progression of prostate cancer. Cancer Res 2006;66:5012–20.
18. van der Kwast TH, Schalken J, Ruizeveld de Winter JA, et al. Androgen receptors in endocrine-therapy-resistant human prostate cancer. Int J Cancer 1991;48:189–93.
19. Ruizeveld de Winter JA, Janssen PJ, Sleddens HM, et al. Androgen receptor status in localized and locally progressive hormone refractory human prostate cancer. Am J Pathol 1994;144:735–46.

TMPRSS2:ERG Fusion by Translocation or Interstitial Deletion Is Highly Relevant in Androgen-Dependent Prostate Cancer, But Is Bypassed in Late-Stage Androgen Receptor – Negative Prostate Cancer

Karin G. Hermans, Ronald van Marion, Herman van Dekken, et al.

Cancer Res 2006;66:10658-10663.